

Characterizing the Sensitivity to Individual Bit Flips in Client-Side Operations of the CKKS Scheme

Matías Mazzanti^{1,2}, Augusto Vega³, Esteban Mocskos^{1,2}

¹*Departamento de Computación, Facultad de Ciencias Exactas y Naturales, Universidad de Buenos Aires (Argentina)*, ²*Centro de Simulación Computacional p/Aplic Tecnológicas (CSC-CONCICET)*, ³*IBM T. J. Watson Research Center (NY, USA)*

Abstract—Homomorphic Encryption (HE) enables computation on encrypted data without decryption, making it a cornerstone of privacy-preserving computation in untrusted environments. As HE sees growing adoption in sensitive applications—such as secure machine learning and confidential data analysis—ensuring its robustness against errors becomes critical. Faults (e.g., transmission errors, hardware malfunctions, or synchronization failures) can corrupt encrypted data and compromise the integrity of HE operations.

However, the impact of soft errors (such as bit flips) on modern HE schemes remains unexplored. Specifically, the CKKS scheme—one of the most widely used HE schemes for approximate arithmetic—lacks a systematic study of how such errors propagate across its pipeline, particularly under optimizations like the Residue Number System (RNS) and Number Theoretic Transform (NTT).

This work bridges that gap by presenting a theoretical and empirical analysis of CKKS’s fault tolerance under single bit-flip errors. We focus on client-side operations (encoding, encryption, decryption, and decoding) and demonstrate that while the vanilla CKKS scheme exhibits some resilience, performance optimizations (RNS/NTT) introduce significant fragility, amplifying error sensitivity.

By characterizing these failure modes, we lay the groundwork for error-resilient HE designs, ensuring both performance and integrity in privacy-critical applications.

Index Terms—Homomorphic encryption; resiliency; soft errors; privacy preservation

I. INTRODUCTION

The need to preserve data privacy becomes critical when processing occurs outside the user’s trusted environment, such as in public clouds or on third-party platforms. In these scenarios, protecting data not only at rest or in transit, but also during processing, is a key challenge.

Homomorphic Encryption (HE) emerges as a promising technique to address this issue. It allows computations to be performed directly on encrypted data without needing to decrypt it first, ensuring confidentiality at all times.

Unlike traditional encryption, which only protects information during storage or transmission, HE enables the secure processing of sensitive data in untrusted environments. For example, it allows a cloud server to calculate statistics on encrypted medical records or train a machine learning model using financial data without revealing its content. In these cases, the server performs the required operations without accessing the plaintext data, preserving its confidentiality throughout the process.

This ability to operate directly on encrypted data is not merely convenient; it is a fundamental requirement for enabling secure computation in infrastructures where full trust cannot be assumed, such as public clouds, third-party platforms, or shared devices. Without such schemes, sensitive applications requiring delegated processing would simply be unfeasible from a privacy standpoint.

Among the most widely used homomorphic schemes is CKKS (Cheon-Kim-Kim-Song), a technique designed for operations on floating-point numbers. This makes it ideal for approximate tasks, such as numerical analysis, signal processing, or machine learning.

To be considered homomorphic, an encryption scheme must be closed under at least addition and multiplication operations on encrypted data. These operations are sufficient to construct any arithmetic circuit, thereby allowing arbitrary computation without needing to decrypt the information. In addition to these fundamental operations, some modern schemes incorporate additional primitives—such as slot rotation or complex conjugation—which, while not increasing the scheme’s expressiveness, are crucial for improving efficiency and facilitating certain computational structures, especially in applications like machine learning.

HE schemes can be divided into three main categories:

- Partially Homomorphic Encryption (PHE) allows for a single type of operation on encrypted data, typically either additions or multiplications. An example is the traditional RSA [1], which supports the multiplication of encrypted data but not addition.
- Leveled Homomorphic Encryption (LHE) supports both operations (addition and multiplication), but only for a finite number of steps before the accumulated noise makes decryption returns corrupted data.
- Fully Homomorphic Encryption (FHE) enables unlimited additions and multiplications, allowing for any arbitrary computation on encrypted data.

Since Craig Gentry’s pioneering proposal [2], numerous studies have optimized the efficiency of HE schemes [3]–[5], improving both their software implementations and acceleration through specialized hardware [6]–[8].

Due to recent advancements in algorithms and optimizations, it has become feasible to ensure that a service provider cannot interpret, transfer, or access users’ encrypted data, even in the event of a security breach. In cryptographic terms, this is achieved because, with appropriate parameters,

breaking a Homomorphic Encryption (HE) scheme becomes a computationally difficult problem. This reinforces confidence in the security of HE and makes its use possible in untrusted environments, such as the public cloud.

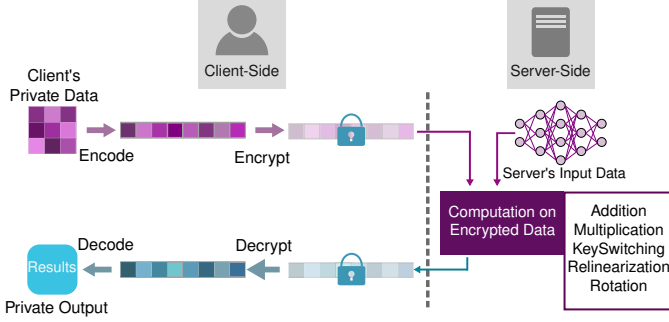


Fig. 1: FHE used in a typical business application: users send their data encrypted with some homomorphic scheme to the cloud, the server operates using the scheme’s operations and returns a result that it is still encrypted.

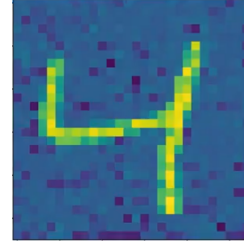
As illustrated in Fig. 1, the typical process for an FHE scheme begins with the user encrypting their data locally using their own key before sending it to the server. The server, in turn, can process this data homomorphically; that is, it performs computations directly on the encrypted data. Once processing is complete, the result, which remains encrypted, is returned to the client, who is solely responsible for its decryption.

The CKKS scheme is gaining an increasing interest in machine learning and data analysis applications due to its ability to perform approximate calculations on floating-point numbers. This characteristic is fundamental for efficiently handling large data volumes and training predictive models, allowing sensitive data to be processed securely without needing decryption. Despite its high computational cost, its potential in these fields continues to be an active area of research and development [9]–[11].

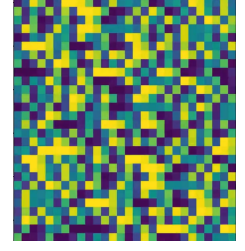
One of the most significant enhancements to the CKKS scheme is using the Residue Number System (RNS) alongside the Number Theoretic Transform (NTT). This combination has helped establish it as a standard and leads to what is known as the full RNS variant [3]. We will refer to this variant simply as CKKS, while the original version without these optimizations will be termed *vanilla CKKS*.

It is crucial to recognize that the CKKS scheme is vulnerable to errors caused by single bit-flips, which can compromise both computational accuracy and data integrity. Since bit-flips may occur under various conditions, assessing their impact on CKKS-based applications—particularly in unreliable hardware environments—is essential.

Figure 2 demonstrates the severe impact of a single bit-flip error in a CKKS-encrypted MNIST image (implemented using `OpenFHE`, a widely adopted FHE library). Despite the ciphertext consisting of millions of bits under standard parameters, flipping just one bit leads to a complete failure in image reconstruction, as evidenced by the corrupted output in Fig. 2(b).



(a) Original



(b) RNS and NTT enabled

Fig. 2: Example of the impact of a single bit-flip in CKKS.

These errors can originate in hardware due to phenomena such as interference, memory failures, or even fault injection attacks [12]–[18], making bit-flip sensitivity analysis a critical aspect for the practical and reliable implementation of HE.

In this work, we conduct a comprehensive analysis of the CKKS scheme’s sensitivity to single-bit errors in client-side stages, such as encoding, encryption, decryption, and decoding operations. We focus on the impact of RNS (Residue Number System) and NTT (Number Theoretic Transform) optimizations on the scheme’s resilience against these errors, exploring an understudied area in the homomorphic encryption literature.

Unlike other proposals focused on specific applications, our analysis provides a general perspective aimed at establishing a clear framework to enhance the security and robustness of CKKS in diverse contexts. Our main contributions are as follows:

- We present the first comprehensive analysis of the CKKS scheme’s sensitivity to individual bit-flip errors in a typical client-side pipeline, considering configurations with and without RNS and NTT optimizations.
- We evaluate the impact of RNS and NTT optimizations on the robustness of the CKKS scheme.
- We identify specific configurations where the use of certain optimizations introduces a form of intrinsic redundancy, increasing the proportion of bits that remain correct in the presence of errors. This finding is particularly relevant for applications where fault tolerance is a fundamental requirement.
- We provide a generalized framework that can serve as a foundation for future research aimed at improving the security and resilience of CKKS against hardware failures.

In the rest of the paper, Section II describes in detail the CKKS scheme in its standard version and its full variant with RNS and NTT. Next, Section III presents a theoretical analysis of CKKS’s robustness against bit-flip errors. Then, Section IV details the methodology used in our experimental campaigns. The experimental analysis is developed in Section V, and finally, Section VI presents the conclusions of the work.

II. BACKGROUND AND CKKS OVERVIEW

In this section, we first introduce the core parameters of the scheme, followed by a conceptual overview alongside a simplified explanation of its key components—making the

material accessible even to readers without a specialized background in cryptography.

We then delve into the mathematical foundations required for the analysis presented in Section III. Readers primarily interested in the experimental methodology may proceed directly to Section IV.

A. General Flow of the CKKS Scheme

CKKS is an approximate homomorphic encryption scheme designed to enable computations on encrypted data while providing explicit control over approximation error. It operates over a polynomial ring of degree N and is based on the Ring Learning With Errors (RLWE) problem, a well-established lattice-based problem that ensures security through the controlled injection of noise into ciphertexts.

CKKS supports the encrypted processing of vectors of real or complex numbers, without ever revealing the original data.

Figure 1 presents the FHE's process consisting of five main stages:

- 1) **Key Generation:** The secret key and public key are generated as degree- N polynomials, created through random sampling and error injection.
- 2) **Encoding:** The input vector is transformed using a specialized inverse Fast Fourier Transform (IFFT) into a degree- N polynomial, constructed such that its evaluations at certain roots of unity approximately reproduce the original values. The resulting polynomial's coefficients are then scaled by Δ and rounded to integers, producing the *plaintext*. Formally, given a polynomial P and a vector $z \in \mathbb{R}^N$, the following relation holds:

$$z = (P(\xi), P(\xi^3), \dots, P(\xi^{2N-1})).$$

A specialized version of the FFT, adapted to the ring $\mathbb{Z}_q[X]/(X^N + 1)$, is used to preserve the algebraic structure of the scheme and enable various optimizations.

- 3) **Encryption:** Given the plaintext, two encrypted polynomials (c_0, c_1) are generated using the public (or secret) key and by adding a small amount of noise. The result $c = (c_0, c_1)$ is referred to as the **ciphertext**.
- 4) **Computation:** Homomorphic operations are performed directly on the ciphertexts, including addition, multiplication, rotations, and other transformations compatible with the scheme.
- 5) **Decryption and Decoding:** The ciphertext is multiplied with the secret key and summed. The result is then divided by Δ , and a specialized FFT is applied to recover an approximation of the original input vector.

Since the security of CKKS relies on the computational hardness of the RLWE problem, each encryption inherently introduces noise. Although it is small at the beginning, it accumulates during homomorphic operations. In general, each operation increases the noise level in the ciphertext, with homomorphic multiplication contributing the most to this growth.

For this reason, the number of successive multiplications is often used as an indirect estimate of the accumulated

error in a ciphertext. If this growth is not properly managed—e.g., through techniques such as bootstrapping—the error can exceed tolerable limits, resulting in incorrect outputs during decryption and decoding.

B. Parameters controlling CKKS

CKKS operates over a polynomial ring defined as:

$$\mathcal{R}_q = \mathbb{Z}_q[X]/(X^N + 1),$$

where \mathbb{Z}_q denotes the integers modulo q , that is, the integer values between 0 and $q - 1$ (addition and multiplication are performed modulo q), $\mathbb{Z}_q[X]$ denotes the polynomials with coefficients in \mathbb{Z}_q , and $/(X^N + 1)$ indicates that polynomials are considered modulo $X^N + 1$.

This ring imposes a negacyclic structure that enables, after encoding, the efficient representation of vectors of complex numbers. In CKKS, data is encoded as a polynomial that, when evaluated at specific values, yields each of the encoded data points. In particular, the degree N must be a power of two and serves two critical purposes: it determines the maximum number of complex values that can be encoded simultaneously ($N/2$), and it is essential for maintaining the security of the scheme.

The original (i.e., vanilla) version of the CKKS scheme uses the following core parameters, which are selected to achieve the desired security level, maintain tolerable error growth, and minimize computational cost:

- N is the ring degree, typically in the range 2×10^{12} to 2×10^{16} , and it determines both the dimension of the encoding space and the computational cost.
- q_0 is the initial modulus—a single large integer (typically up to 60 bits)—that largely defines the target precision.
- Δ is the scaling factor, a constant used to amplify real values before encoding in order to preserve floating-point precision.
- L is the multiplicative depth, that is, the number of homomorphic multiplications that can be performed before accumulated noise degrades precision.

The total modulus of the scheme, denoted Q , and the size of the coefficients in the encoding and encryption polynomials are defined differently depending on the CKKS variant used. In the vanilla version, Q is given by:

$$Q = \Delta^L \cdot q_0,$$

In CKKS, each multiplication between ciphertexts increases both the error and the magnitude of the encoded values. To control this growth and preserve precision, an operation called *rescaling* is applied. Rescaling reduces the scale of the encoded values and also decreases the active modulus, which in turn limits the number of consecutive multiplications (with rescaling) that can be performed. This limit is known as the **multiplicative depth** of the scheme. The parameter Δ is applied L times—once for each multiplicative level supported by the modulus hierarchy.

1) *CKKS full RNS variant*: The **Residue Number System** (RNS) is an alternative representation of integers that expresses a number through its residues modulo several small, pairwise coprime integers. This encoding allows arithmetic operations—such as addition and multiplication—to be performed independently and in parallel on each modulus, reducing computational complexity and significantly improving efficiency. These properties make RNS particularly well-suited for high-performance contexts such as homomorphic encryption.

The use of the **Chinese Remainder Theorem** (CRT) is essential in RNS, as it ensures that each set of residues uniquely corresponds to a single integer within a defined range. Moreover, CRT provides an efficient way to reconstruct the original integer from its residue representation.

In the RNS-optimized variant of the CKKS scheme, all polynomials involved (i.e., messages, keys, and ciphertexts) are represented as multiple polynomials of the same degree, one for each residue modulo in the RNS base. Additionally, each of these polynomials is transformed using the Number Theoretic Transform (NTT)—a modular analogue of the Fast Fourier Transform (FFT). NTT accelerates polynomial multiplication, which is one of the most computationally intensive operations in the scheme.

These optimizations—RNS and NTT—do not alter the semantics of the encryption scheme but do change its internal implementation. In particular, they have implications for error propagation and sensitivity, topics that will be analyzed in detail in Section III.

In this variant, the total modulus of the scheme is expressed as:

$$Q = \prod_{i=0}^{L-1} q_i, \quad (1)$$

where q_0 is the initial modulus and q_1, \dots, q_L are additional moduli that in general are selected by the scheme, all of similar bit length. It is worth noting that some libraries provide manual control over the bit-length of these q_i moduli, the implementations employed in this work automatically configure these parameters according to the bit length specified for q_0 .

C. CKKS' Insights

The CKKS scheme accepts as input a vector of up to $N/2$ floating-point elements, i.e., $\in \mathbb{C}^{N/2}$. This input is mapped into the polynomial ring $\mathbb{Z}[X]/(X^N + 1)$ through a process known as encoding, producing a plaintext polynomial m . Here, $\mathbb{Z}[X]$ denotes the ring of polynomials with integer coefficients, and $\mathbb{Z}[X]/(X^N + 1)$ is the quotient ring where polynomials are reduced modulo $X^N + 1$. This implies working with polynomials of degree at most $N - 1$ under negative (or negacyclic) convolution. In this context, polynomial reduction is performed via the substitution $X^N = -1$, ensuring that results remain within the allowed polynomial space of degree less than N .

The resulting plaintext is then encrypted using either the public or secret key, following the RLWE problem, where a small amount of noise is intentionally injected for security. The ring $\mathbb{Z}[X]/(X^N + 1)$ is preferred in RLWE-based schemes due

to its stronger security properties compared to $\mathbb{Z}[X]/(X^N - 1)$, where the convolution is cyclic and considered more vulnerable to attacks.

a) *Precision*: To better understand the parameter selection in CKKS, it is helpful to clarify the concept of precision. In the case of OpenFHE with real-valued inputs only, the scaling parameter Δ determines how many bits are used to encode the fractional part of the input values, while the difference between the initial modulus q_0 and Δ indicates the number of bits allocated to the integer part.

For example, using $q_0 = 60$ bits y $\Delta = 50$ bits allows the encrypted representation of real numbers with approximately 10 bits of precision for the integer part and 50 bits for the fractional part.

b) *Keys*: Encryption in the CKKS scheme requires either a secret key sk or a public key pk . The secret key is generated by sampling a vector s of length N generally from a ternary distribution with Hamming weight h , and then setting $sk = (1, s)$.

The public key is constructed by sampling a_0 from \mathbb{Z}_Q , i.e., from the set of positive integers less than the modulus Q , and an error term e_0 from a discrete Gaussian distribution with standard deviation $\sigma = 3.2$. The public key is then defined as:

$$pk = ([-a_0s + e_0]_Q, a_0) = (p_0, p_1)$$

where the notation $[\dots]_Q$ denotes reduction modulo Q .

c) *Encoding*: The key idea behind encoding in CKKS is to transform the input vector into a polynomial. Different libraries implementing CKKS vary in how they perform this transformation using IFFT/FFT-based methods. In all cases, the standard cyclic transform must be adapted to a negacyclic version to ensure operations remain within the ring $\mathbb{Z}_q[X]/(X^N + 1)$ used by the scheme.

The transforms employed by HEAAN 1.0 and OpenFHE 1.2.3 are negacyclic and include scheme-specific optimizations, commonly referred to as specialized FFT/IFFT. These versions incorporate several improvements originally proposed by Bernstein [19], [20]. One of their main advantages is that they allow the transform to be applied directly to vectors of size $\leq N/2$, without expanding them to size N , which significantly reduces computational cost.

Given a real-valued input vector of size $n \leq N/2$, the encoding process begins by padding the vector with zeros to reach the next power of two, denoted n' . A specialized inverse FFT is then applied, producing a complex vector of length n' . From this, a polynomial of degree $N - 1$ is constructed.

First, the gap parameters $= \frac{N/2}{n'}$ is computed, and the lower half of the polynomial (coefficients of degree 0 to $N/2 - 1$) is filled with the real parts of the transformed vector, with assignments spaced at intervals of size *gap*. Unassigned coefficients are set to zero.

Finally, as is illustrated in Fig. 3, each coefficient is multiplied by Δ , and then rounded to the nearest integer using the coordinate-wise randomized rounding method described in [21].

d) *Encryption*: The encryption of a plaintext m using the secret key $sk = (1, s)$ and modulus Q is given by:

$$c_{sk} = ([m + a \times s + e]_Q, [-a]_Q) = (c_0, c_1) \quad (2)$$

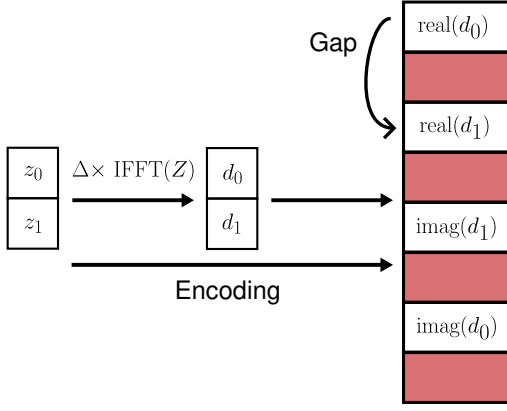


Fig. 3: Encoding scheme in CKKS using HEAAN/OpenFHE. The example shows an input vector with $n = 2$ values, represented in a polynomial ring of size $N = 8$, where the gap between consecutive coefficients is 2.

where a is a polynomial sampled from a uniform distribution, e is a noise term sampled from a discrete Gaussian distribution, and the notation $[\cdot]_Q$ denotes reduction modulo Q .

An alternative way is encrypting by using the public key, $pk = (p_0, p_1)$. In this case, encryption is defined as:

$$c_{pk} = ([m + p_0 \times v + e_1]_Q, [p_1 \times v + e_2]_Q) = (c_0, c_1) \quad (3)$$

where v is an ephemeral (one-time) polynomial sampled from a ternary distribution, and e_1, e_2 are error terms sampled similarly to e in the previous procedure.

e) *Decryption*: Decryption in both cases (secret key and public key encryption) uses the secret key $sk = (1, s)$ and the encrypted text (c_0, c_1) as follows:

$$m' = [c_0 + c_1 \times s]_Q \quad (4)$$

f) *Decoding*: To decode a plaintext polynomial m with N coefficients, one must reconstruct a complex-valued vector of n' elements by reversing the encoding process illustrated in Fig. 3. The i -th element ($i \leq N/2$) of the resulting vector is formed by using the real part of the i -th coefficient of the plaintext, and the imaginary part from the coefficient at position $i + N/2$.

This complex vector is then divided by Δ , and a specialized FFT is applied to recover the approximate original input.

Due to rounding effects during encoding and decoding, the final result may contain small approximation errors. Corollary 3 in [22] shows that the worst-case distance between the input vector z and the output vector z' (after encoding and decoding) at each position is approximately: $N/(\pi \times \Delta)$.

With a sufficiently large Δ , this difference becomes negligible. Given that a typical ring size N ranges from 2×10^{12} to 2×10^{16} , using a scaling factor on the order of 2^{20} is enough to ensure a reasonable approximation error. In our case, since we use a smaller N for practical reasons, the approximation error is even smaller and can be considered negligible.

g) *Security Against Secret Key Attacks*: To defend against secret key recovery attacks, OpenFHE performs additional operations before applying the specialized FFT during the decoding process. Specifically, a Gaussian error is injected

prior to this step, with its standard deviation determined by the vector being decoded. This mechanism is critical: in our bit-flip experiments—when security analysis is not disabled—the software throws an exception during this stage, resulting in premature termination of execution.

This behavior demonstrates the role of these protective measures in preventing potential side-channel or fault-injection attacks that could compromise the secret key.

D. RNS and NTT Optimizations

In the full RNS/NTT variant of CKKS [3], the Residue Number System (RNS) is used to split large polynomial coefficients into multiple smaller values, enabling more efficient computations. This approach allows arithmetic in \mathbb{Z}_Q to be performed using standard machine word sizes, by working with small moduli that simplify computation.

The magnitude of the modulus Q can range from hundreds to thousands of bits, depending on the use case. However, modern computing systems typically operate with word sizes of 64 bits or less, making direct operations on such large coefficients impractical. To address this, polynomials (keys, plaintexts, ciphertexts) are represented using an equivalent decomposition in the RNS form. Each coefficient is represented modulo a small prime q_i , to generate Q like Eq. 1

This decomposition enables addition and multiplication in \mathbb{Z}_Q using standard machine word operations. All other parameters, as well as the encoding and decoding procedures, remain consistent with the vanilla CKKS variant.

Polynomial multiplications are performed efficiently using the Number Theoretic Transform (NTT), which reduces the computational complexity of the operation from $\mathcal{O}(n^2)$ to $\mathcal{O}(n \log n)$. Addition of polynomials and multiplication by a scalar are both $\mathcal{O}(n)$ operations in both the coefficient and evaluation (NTT) representations.

By default, the CKKS scheme assumes that polynomials are represented in the NTT domain (evaluation representation). When certain operations require polynomials in coefficient form, an inverse NTT (iNTT) is applied to transform ciphertexts from the evaluation domain back to the coefficient domain. However, within the scope of this work, as all computations are performed on the client side, this change of representation does not occur.

The procedures for encoding, encryption, decryption, and decoding remain virtually unchanged, except that all operations are now performed using the RNS and NTT representations.

III. ERROR RESILIENCE ANALYSIS

This section presents a theoretical analysis of the error induced by a single bit-flip at different stages of the CKKS scheme. We address both the vanilla and the full RNS variant versions. Our aim is:

- Deriving analytical bounds in the case without RNS or NTT.
- Identifying the most sensitive coefficients.
- Providing an intuitive description of error behavior in practical implementations.

Although a closed-form analytical bound can not be derived for the full RNS variant version due to the complexity of modular representations, a qualitative analysis of the observed patterns is provided.

A. Error Model for a Single Bit-Flip

We adopt a single bit-flip model, where a single bit is altered. In practice, such faults may be caused by electromagnetic interference, hardware failures, or cosmic rays [12], [13], [15], [17], [23], [24].

Let p be the original value of a coefficient, either in a plaintext polynomial \mathbf{m} or in one of the ciphertext polynomials (c_0, c_1) . We denote this generic polynomial as \mathbf{p} . Let's p'_j be the result of flipping a bit j of p , then the resulting error is:

$$e_j = p'_j - p \quad (5)$$

We model this fault as an error vector $\mathbf{e}_{i,j} \in \mathbb{R}^N$ whose only non-zero component corresponds to bit j of coefficient i :

$$\mathbf{e}_{i,j} = (0, \dots, 0, e_j, 0, \dots, 0) \quad (6)$$

This model enables us to track how a single bit-flip propagates through the cryptographic pipeline.

B. CKKS Encoding via DFT

As discussed in Section II, one of the key components of encoding and decoding in CKKS is FFT. Although CKKS uses a specialized inverse FFT for computational efficiency, this transformation is typically implemented using optimized algorithms that obscure its underlying linear structure.

Instead, we rely on the negacyclic Discrete Fourier Transform (DFT)—an algebraically equivalent transformation explicitly expressed as matrix multiplication. This formulation allows us to:

- 1) Directly represent how errors propagate through the encoding process.
- 2) Analyze the isolated effect of a perturbation in a single coefficient.
- 3) Derive analytical bounds on the magnitude of the error without dealing with the internal optimizations of FFT implementations.

While this choice sacrifices performance, it offers significant pedagogical advantages, allowing for an intuitive understanding of how bit-flip errors are amplified or distributed during encoding.

1) *Encoding via Negacyclic DFT:* Let $M = 2N$ and $\xi = e^{-2\pi i/M}$. To construct a negacyclic Discrete Fourier Transform (DFT), we evaluate it at the odd powers of the roots of the cyclotomic polynomial $\Phi_M(X) = X^N + 1$; that is, at $\xi^1, \xi^3, \xi^5, \dots, \xi^{2N-1}$. We define the **Vandermonde matrix** where each column corresponds to a different power of these roots of unity:

$$W = \begin{pmatrix} \xi^{1 \cdot 0} & \xi^{1 \cdot 1} & \dots & \xi^{1 \cdot (N-1)} \\ \xi^{3 \cdot 0} & \xi^{3 \cdot 1} & \dots & \xi^{3 \cdot (N-1)} \\ \vdots & \vdots & \ddots & \vdots \\ \xi^{(2N-1) \cdot 0} & \xi^{(2N-1) \cdot 1} & \dots & \xi^{(2N-1) \cdot (N-1)} \end{pmatrix} \quad (7)$$

and we denote its inverse as W^{-1} , which is required for the encoding process. Due to the properties of this matrix, its inverse is simply the conjugate transpose (Hermitian transpose) normalized by N :

$$W^{-1} = \frac{1}{N} W^\dagger$$

In order to use the DFT and its inverse for encoding to obtain results equivalent to those produced by implementations such as HEAAN and OpenFHE, some preprocessing is required: the input vector must be resized to length N and reordered to satisfy the requirements of those systems. However, these adjustments do not affect the behavior of the error model under analysis and will be omitted for simplicity.

In general, for an input vector of $n \leq N/2$ elements, it is first zero-padded to length $N/2$, and then mirrored with its complex conjugate to reach a total length of N . Once the input vector $\mathbf{z} \in \mathbb{R}^N$ is prepared and reordered, the encoding proceeds as follows:

$$\begin{aligned} \text{Encode}(\mathbf{z}) &= \text{Round}(W^{-1}(\Delta \mathbf{z})) \\ &= \text{Round}(\Delta \cdot W^{-1} \mathbf{z}) = \mathbf{m} \in \mathbb{Z}^N, \end{aligned} \quad (8)$$

where Δ is the already defined scaling factor. Due to the Hermitian symmetry of W and W^{-1} , and the conjugate extension of the input, the result of $W^{-1} \mathbf{z}$ lies entirely in the real subspace.

To recover an approximation of the original input \mathbf{z} from \mathbf{m} , decoding is performed as:

$$\text{Decode}(\mathbf{m}) = \mathbf{z}' = W(\mathbf{m}/\Delta) \quad (9)$$

Finally, the output undergoes the same reordering process as in encoding, and the n components of \mathbf{z}' are extracted. Since the DFT output is complex-valued while OpenFHE supports only real-valued encryption, the real part is extracted to obtain the final approximation of \mathbf{z} .

C. Theoretical Estimation of Encoding Error in Vanilla CKKS

This section focuses on the impact of single-bit errors during the encoding phase of the CKKS scheme.

Let us consider the case in which an error $\mathbf{e}_{i,j}$ is introduced by flipping a single bit in coefficient i of the plaintext vector \mathbf{m} , specifically at the j -th bit position. The resulting perturbed plaintext is $\mathbf{m}' = \mathbf{m} + \mathbf{e}_{i,j}$, and decoding proceeds as in Eq. 9:

$$\begin{aligned} \mathbf{z}'' &= W \times \frac{\mathbf{m}'}{\Delta} = W \times \frac{\mathbf{m} + \mathbf{e}_{i,j}}{\Delta} \\ &= W \times \frac{\mathbf{m}}{\Delta} + W \times \frac{\mathbf{e}_{i,j}}{\Delta} \\ &= \mathbf{z}' + W \times \frac{\mathbf{e}_{i,j}}{\Delta} \end{aligned}$$

Since a single bit-flip affects only one coefficient, the resulting error is localized. The difference between the decoded vectors \mathbf{z}' and \mathbf{z}'' is given by:

$$\|\mathbf{z}' - \mathbf{z}''\| \propto \|W \times \mathbf{e}_{i,j}/\Delta\| \quad (10)$$

1) *Bit-Flip Injection during Encoding*: To better understand the analytical expression of the error in Eq. (10), we simulate flipping each individual bit in the plaintext coefficients. Let $j \in \{0, \dots, 63\}$ denotes the bit position in a 64-bit unsigned integer. For each iteration, we flip the j -th bit of a coefficient, introducing an error with integer magnitude $e_j = 2^j$. This represents the maximum jump in value induced by flipping bit j in a coefficient, which is stored as an unsigned integer—as in the case of plaintext coefficients.

We repeat this process for all coefficients, grouping the results into $N = 4$ blocks of 64 iterations each, and use $\Delta = 2^{50}$. Let \mathbf{z}' be the decoded vector without errors, and \mathbf{z}'' the result after applying the bit-flip and decoding. Using Eq. (10), we define:

$$L_2(i, j) = \|\text{Real}(W \times \mathbf{e}_{i,j}/\Delta)\|_2 \quad (11)$$

where $\mathbf{e}_{i,j}$ is a zero vector of length N with value e_j at position i .

We also take the real part of the vector before computing the L2 norm, to simulate the encoding of real-valued data, as in OpenFHE, in contrast to HEAAN, which allows complex inputs. This step is important not only to maintain consistency with the backend used in later sections, but also because it exposes a specific behavior that would otherwise not manifest when keeping the complex part.

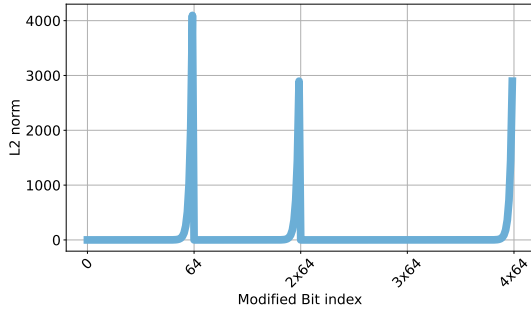


Fig. 4: L_2 norm of the error after a single bit-flip in the plaintext during encoding. The horizontal axis shows the bit-flip position $i * 64 + j$, and the vertical axis shows $L_2(i, j)$. Ring dimension $N = 4$; scaling factor $\Delta = 2^{50}$.

Figure 4 shows the values of $L_2(i, j)$ as a function of the bit-flip position. $L_2(i, j)$ grows exponentially with j for each coefficient i , consistent with the 2^j dependency. An exception appears at $i = N/2 = 2$, where the norm remains zero. This occurs because, in the DFT, the coefficient at index $N/2$ contributes only imaginary components, which vanish when taking the real part of the transform.

2) *Effect of the Scaling Factor on Bit-Flip Error*: To explore how the scaling factor Δ affects the magnitude of bit-flip errors, we repeat the previous experiment using different values of $\Delta \in \{2^{20}, 2^{40}, 2^{50}\}$. For each case, we plot $L_2(i, j)$ using a semi-logarithmic scale on the y -axis for easier comparison.

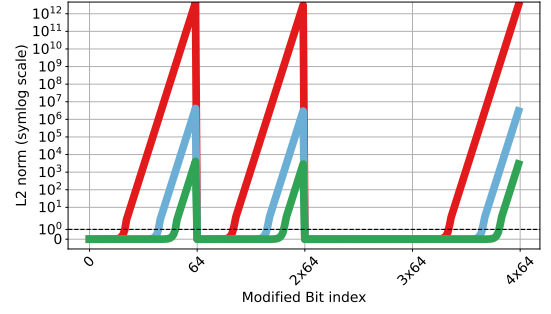


Fig. 5: L_2 norm of the error after a single bit-flip in the plaintext during encoding, for various scaling factors Δ . The horizontal axis indicates the bit position j ; the vertical axis is in semi-log scale. Ring dimension: $N = 4$.

As shown in Fig. 5, increasing Δ significantly reduces the error magnitude and increases the number of *resilient* bits. This occurs because the impact of errors becomes noticeable only when the flipped bit corresponds to or exceeds the magnitude of Δ . In other words, the larger the scaling factor, the more initial bits remain unaffected, yielding smaller error norms and higher bit-level fault tolerance.

This empirical observation is analytically confirmed by equation 11, which shows that the error is inversely proportional to the scaling factor. When an error $e_{i,j}$ is divided by Δ , noise components with magnitudes smaller than the bit precision of Δ are effectively suppressed in the final result. This mathematical relationship explains why larger scaling factors provide enhanced fault resilience: they act as a natural filter that attenuates the impact of small-magnitude bit flips on the decoded output.

However, this resilience comes at the cost of reduced fractional precision in the encoded message (see Section II). The selection of Δ therefore requires careful consideration of the trade-off between error tolerance and numerical precision, balancing the competing demands of fault resilience and computational accuracy.

D. Theoretical Estimation of Error during Encryption using Vanilla CKKS

This section analyzes three scenarios involving a single bit-flip in vanilla CKKS:

- 1) A bit-flip in the plaintext (before encryption).
- 2) A bit-flip in the ciphertext (in one of the ciphertext polynomials).
- 3) A bit-flip in the plaintext (before decoding).

Under public-key encryption, a plaintext vector \mathbf{m} is encoded into a polynomial $\mathbf{m}(X)$, encrypted as in Eq. 3, and decrypted using Eq. 4.

1) *Bit-Flip in the Plaintext Before Encryption*: Suppose a bit-flip introduces an error $\mathbf{e}_{i,j}$ in the i -th coefficient at bit position j , so the plaintext becomes:

$$\mathbf{m}' = \mathbf{m} + \mathbf{e}_{i,j}, \quad \mathbf{e}_{i,j} = e_j X^{i-1} \quad (12)$$

Encrypting \mathbf{m}' using the public key (as in Eq. 3) yields:

$$\begin{aligned} ct' &= ([\mathbf{m}' + p_0 v + e_1]_Q, [p_1 v + e_2]_Q) \\ &= ([\mathbf{m} + e_j X^{i-1} + p_0 v + e_1]_Q, c_1) = (c'_0, c_1). \end{aligned} \quad (13)$$

The error affects only the ciphertext component c'_0 in coefficient i , with a maximum magnitude $|e| \leq Q/2$ due to modular arithmetic. Upon decryption (using Eq. 4):

$$\mathbf{m}'' = [c'_0 + c_1 s]_Q = \mathbf{m} + e_j X^{i-1} + (e_1 + e_2 s) \quad (14)$$

However, the error magnitude grows exponentially with the flipped bit position, as each bit represents a successive power of 2 in the binary representation. Consequently, an exhaustive bit-flip analysis across all coefficient positions, with L2 norm computation for each perturbation, yields the exponential error scaling pattern illustrated in Fig. 4 (Section III-C). that the bit-flip impact remains localized to the position i and scales linearly with e_j .

The error induced by the bit-flip affects only the ciphertext component c'_0 in coefficient i , with a maximum magnitude $|e| \leq Q/2$ due to modular arithmetic. Decoding this plaintext will therefore produce an error consistent with that discussed in Section III-C.

2) *Bit-Flip in the Ciphertext*: If the bit-flip occurs in the ciphertext, two sub-cases arise:

a) *Flip in c_0* : For a perturbed ciphertext $ct' = (c_0 + e_j X^{i-1}, c_1)$, the behavior mirrors the previous plaintext case: the error remains localized in coefficient i and results in a decoding error proportional to e_j .

b) *Flip in c_1* : For a perturbed ciphertext $ct' = (c_0, c_1 + e_j X^{i-1})$, decryption proceeds as:

$$\begin{aligned} \mathbf{m}'' &= [c_0 + (c_1 + e_j X^{i-1}) s]_Q \\ &= [(c_0 + c_1 s) + (e_j X^{i-1} s)]_Q \\ &= [(\mathbf{m} + e_1 + e_2 s) + (e_j X^{i-1} s)]_Q \end{aligned}$$

where $e_j X^{i-1} s$ involves polynomial multiplication. Thus, the error spreads across all N coefficients. Since the secret key s has small coefficients (much less than q_0), each coefficient in the result incurs an error of magnitude proportional to e_j , but this error is now distributed. The maximum magnitude is bounded by $|e_j| \cdot \|s\|_\infty$.

3) *Bit-Flip in the Plaintext Before Decoding*: If a bit-flip is introduced in coefficient i of a plaintext \mathbf{m} , after decryption but before decoding, the effect is analogous to the case analyzed in Section III-C. This follows directly since the plaintext being decoded is equivalent to:

$$\mathbf{m}' = \mathbf{m} + e_j X^{i-1} \quad (15)$$

which is the same structure previously analyzed.

E. Theoretical Estimation of Error in RNS

CKKS typically uses a Residue Number System (RNS) representation for the modulus $Q = \prod_{k=0}^{L-1} q_k$, where L determines the number of available levels (i.e., number of supported homomorphic operations).

Each coefficient $p \in \mathbb{Z}_Q$ is represented by its residues:

$$r_k = p \bmod q_k \quad \text{for } k = 0, \dots, L$$

When applied to all coefficients of a polynomial (from an encoded message or ciphertext), this yields L **residue polynomials**, commonly referred to as **limbs**. Reconstruction

via the Chinese Remainder Theorem (CRT), as shown in Mohan [25, Chapter 5], is:

$$p = \left(\sum_{k=1}^L r_k \left[\left(\frac{1}{Q_k} \right) \bmod q_k \right] Q_k \right) \bmod Q \quad (16)$$

where

$$Q_k = Q/q_k$$

and $\frac{1}{Q_k}$ are the multiplicative inverse of Q_k .

A bit-flip on the j bit affecting the k -th residue changes it to $r'_k = r_k + e_{k,j}$, which introduces an error into the reconstructed value:

$$p' = p + e_{k,j} Q_k \left[\left(\frac{1}{Q_k} \right) \bmod q_k \right] \pmod{Q} \quad (17)$$

This error can be as large as Q_k , potentially spanning hundreds or thousands of bits, even though the bit-flip affected only one bit in a single residue.

F. Theoretical Estimation of Error in NTT

To accelerate encoding and decoding operations, CKKS uses the Negacyclic Number Theoretic Transform (NTT) over the ring $\mathbb{Z}_q[X]/(X^N + 1)$. Let $\psi \in \mathbb{Z}_q$ be a primitive $2N$ -th root of unity satisfying:

$$\psi^2 \equiv \xi, \quad \psi^N \equiv -1 \pmod{q},$$

where ξ is a primitive N -th root of unity. The NTT matrix is then defined as:

$$W_{NTT} = \begin{pmatrix} \psi^{2(0 \times 0) \cdot 0} & \psi^{2(0 \times 1) \cdot 1} & \dots & \psi^{2(0 \times N-1) \cdot N-1} \\ \psi^{2(1 \times 0) \cdot 0} & \psi^{2(1 \times 1) \cdot 1} & \dots & \psi^{2(1 \times N-1) \cdot N-1} \\ \psi^{2(2 \times 0) \cdot 0} & \psi^{2(2 \times 1) \cdot 1} & \dots & \psi^{2(2 \times N-1) \cdot N-1} \\ \vdots & \vdots & \ddots & \vdots \\ \psi^{2(N-1 \times 0) \cdot 0} & \psi^{2(N-1 \times 1) \cdot 1} & \dots & \psi^{2(N-1 \times N-1) \cdot N-1} \end{pmatrix}$$

We denote its inverse as W_{NTT}^{-1} . When a single bit-flip occurs at bit position j within coefficient i , the induced perturbation after NTT transformation becomes:

$$\mathbf{m}' - \mathbf{m} = W_{NTT} \mathbf{e}_{i,j}.$$

Therefore, the L_2 norm of the error is:

$$\|\mathbf{m}' - \mathbf{m}\|_2 = \|W_{NTT} \mathbf{e}_{i,j}\|_2.$$

This behavior parallels that of the Discrete Fourier Transform (DFT), except that the NTT operates over \mathbb{Z}_q with moduli q typically of 30 bit to 60 bit. The twiddle factors, being roots of unity modulo q , can amplify errors during the transformation, thereby increasing the error magnitude.

Figure 6 shows the values of $L_1(i, j)$ for $N = 4$ and 64-bit coefficients in the NTT case. The horizontal axis indicates the bit-flip position $i \cdot 64 + j$, and the vertical axis shows $L_2(i, j)$ on a logarithmic scale.

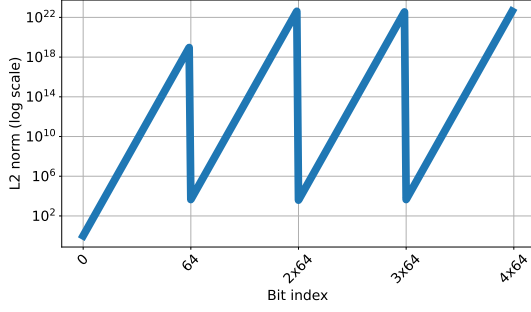


Fig. 6: L_2 norm of the error after a single bit-flip in the plaintext during encoding. The horizontal axis shows the modified bit position $i * 64 + j$; the vertical axis shows the $L_2(i, j)$ norm on a logarithmic scale. Ring dimension: $N = 4$.

As the Fig. 6 shows, even the flips in the least significant bits cause the norm to exceed four orders of magnitude—producing errors large enough to make correct decoding practically impossible, as will be further illustrated in Section V.

G. Summary

The following points summarize the theoretical impact of a single bit-flip at different stages of the CKKS encryption pipeline, both in its vanilla and optimized implementations:

- **Bit-flip in the plaintext before encryption:** the error remains localized in a single coefficient where the bit-flip occurred, with a magnitude proportional to $e_j = 2^j$, depending on the flipped bit's position j .
- **Bit-flip in the ciphertext (c_0):** identical to the plaintext case—the error remains localized after decryption, with magnitude again proportional to the bit position j .
- **Bit-flip in the ciphertext (c_1):** the error is multiplied by the secret key s , becoming distributed across all N coefficients; its maximum magnitude is $\mathcal{O}(e_j \|s\|_\infty)$.
- **Bit-flip in the plaintext before decoding:** behaves like a localized error in a single coefficient of the encoded polynomial—effectively equivalent to the encoding case, plus minor encryption noise.
- **RNS:** a bit-flip in a single *limb* (residue) can result in a reconstruction error of order $\mathcal{O}(Q_k)$, where $Q_k = Q/q_k$ is typically a large value.
- **Negacyclic NTT:** a bit-flip before or after the NTT produces an error proportional to $W_{NTT} e_{i,j}$, spreading across all coefficients. Entries of W_{NTT} are bound by modulus q , which typically ranges from 30 bit to 60 bit, thus potentially amplifying the error significantly.

IV. EXPERIMENTAL DESIGN

This section describes the experimental design used to quantify the resilience of the CKKS homomorphic encryption scheme under single bit-flip fault injections.

A. Test Environment

All experiments were executed on the same machine (Intel i7-11700, 32GB, Arch Linux 257.5-1).

Two different implementations of CKKS were used to cover both the vanilla and optimized variants of the scheme:

- **HEAAN 1.0:** a vanilla implementation without RNS or NTT, using arbitrary-precision coefficients managed by the NTL library (a C++ library for number theory and arbitrary-precision arithmetic).
- **OpenFHE 1.2.3:** a modular implementation with native support for RNS and NTT, using 64-bit internal coefficients (`uint64`).

Although more recent versions of HEAAN include RNS and NTT optimizations, version 1.0 allows a cleaner comparison to a vanilla CKKS. Conversely, OpenFHE represents the optimized variant, due to its widespread use in the field of homomorphic encryption [26] and its active support for high-performance execution environments.

Minor modifications were made to both libraries to gain full control over the selection of pseudo-random number generator (PRNG) seeds. This ensured strict reproducibility of experiments and allowed for precise isolation of the effects caused by each individual bit-flip.

In the case of HEAAN 1.0, we have these additional implementation details:

- The bit-length of each coefficient is not fixed in advance; it depends on internal combinations of q_0 and Δ , and may vary depending on the PRNG seed used by the scheme.
- Due to NTL implementation, bits larger than Q are ignored in internal operations, which limits the scope of bit-level analysis.

OpenFHE has the following implementation details:

- Uses 64-bit integer coefficients (`uint64_t`) without arbitrary-precision arithmetic.
- The initial modulus q_0 can be explicitly configured by the user. This parameter determines the starting bit-level precision of the scheme. The subsequent moduli q_i are automatically selected to match the bit length of q_0 , ensuring uniform precision across levels.
- The total number of moduli depends on the required multiplicative depth of the computation.
- Public APIs for accessing and modifying coefficients at each pipeline stage (i.e., encoding, encryption, etc.).
- Enables injection of fixed-length bit-flips (up to 64 bits) at controlled and reproducible positions.
- Supports 128-bit arithmetic, which—though not used in this work—offers a pathway for future experiments.

B. Using OpenFHE as Vanilla CKKS implementation

OpenFHE is significantly more computationally efficient than HEAAN. However, it does not natively offer a mechanism to disable RNS and NTT optimizations. To address this, we devised a procedure to emulate a vanilla CKKS scheme within OpenFHE by explicitly bypassing both RNS and NTT optimizations, despite their built-in support in the library:

- **RNS:** We enforced a single-limb representation, which is feasible for depth-zero operations (i.e., no ciphertext multiplications). Additionally, automatic rescaling was disabled and replaced with manual scaling to prevent the introduction of additional limbs.

- **NTT:** Prior to injecting a bit-flip, the polynomial is transformed from evaluation space back to coefficient space via inverse NTT (INTT). We flip the desired bit and transform the polynomial back to the evaluation space using NTT. After this hook, the pipeline continues normally.
- **Limitations of disabling NTT:** Since the NTT operates modulo q_0 , flipping bits beyond the bit-width of q_0 causes modular wraparound, which can alter the intended effect of the bit-flip and potentially lead to catastrophic decryption errors. To minimize distortion in the analysis, we set q_0 to the maximum value supported by the library—60 bits—ensuring that most bit-flips occur within the valid range and reducing unintended side effects from modular arithmetic.

C. Internal Error Detection in OpenFHE

OpenFHE includes an internal consistency check that estimates the standard deviation of the imaginary part of the decoded *plaintext*, designed to detect potential secret key leakage attacks. Flipping high-order bits at different stages of the homomorphic pipeline can result in large deviations, triggering this mechanism and aborting the decoding. To isolate the analysis of numerical resilience, we disable this mechanism.

This methodology enables controlled and reproducible exploration of both vanilla and optimized CKKS configurations, allowing for a rigorous assessment of the impact of single-bit faults at various stages of the homomorphic pipeline.

D. Vanilla CKKS over OpenFHE Validation

To ensure that OpenFHE’s vanilla mode faithfully replicates the behavior of HEAAN 1.0, we follow these validation steps:

- 1) Configure OpenFHE in vanilla mode (not using RNS and NTT) and set q and Δ to match HEAAN’s effective bit precision.
- 2) Restrict input values in HEAAN to real numbers, in line with OpenFHE’s plaintext constraints.
- 3) Compare L_2 norms and error statistics after identical bit-flips in both libraries.
- 4) Verify consistent sensitivity patterns across low- and high-order bit positions.

E. Input Vector Generation and PRNG Control

Since our analysis is not tied to any specific application, the input data consists of real-valued vectors with uniformly distributed random entries. To evaluate the sensitivity of CKKS, we define input ranges using power-of-two boundaries and sample values uniformly within these intervals.

A wider input range affects the signal-to-noise ratio by increasing the difference between the smallest and largest representable values.

Unless otherwise specified, input values are sampled as uniformly distributed real numbers within the interval 0 to 256, and represented in double-precision floating-point format.

The bounded input range allows us to test multiple Δ , allowing for a more comprehensive analysis of their impact on encoding and rounding errors. By varying Δ across a wide range without exceeding coefficient bounds, we can better understand the trade-offs between precision and noise growth, as discussed in Section II-B.

To evaluate stability with respect to seed variation, each experiment (i.e., each individual bit-flip) is repeated 2500 times. Each repetition involves 100 different seeds for the scheme PRNG and 25 for the input generator. These seed combinations are fixed and shared across all experiments, ensuring that results could be compared under equivalent input conditions.

Although this number of repetitions may not suffice for exhaustive statistical inference, our tests show very low variability, confirming it is enough for the aims of this study.

F. Bit-Flip Injection Procedure

Error injection is performed by flipping a single bit in one encrypted coefficient during each execution. The general workflow for the experiments is as follows:

- 1) Encode and, if applicable, encrypt the input vector using the selected library.
- 2) (If required) Apply the inverse NTT (INTT) to bring the plaintext or ciphertext into coefficient space.
- 3) Flip a single bit within one coefficient (64-bit precision in OpenFHE; arbitrary-precision in HEAAN).
- 4) (If required) Reapply NTT to return to evaluation space.
- 5) Proceed with the homomorphic operation pipeline.
- 6) Decrypt and decode the result.
- 7) Compute evaluation metrics.

This process is performed once per bit and coefficient across both *plaintext* and *ciphertext* scenarios in separate experiments. The entire procedure was repeated for each seed combination.

In OpenFHE, we test configurations both with and without RNS and NTT by dynamically disabling these optimizations at runtime. This allows direct comparisons between the optimized and vanilla implementations, isolating the impact of each optimization technique.

G. Evaluation Metrics

Given the original decrypted vector \mathbf{x} (without bit-flips) and the resulting vector \mathbf{y} after error injection and decryption, we quantify the deviation introduced by each bit-flip by two complementary evaluation metrics:

a) *Mean Squared Error (MSE)*: The element-wise error is defined as:

$$\delta_i = y_i - x_i$$

and the MSE is computed as:

$$\text{MSE} = \sqrt{\frac{1}{k} \sum_{i=1}^k \delta_i^2}$$

b) *Element-wise Relative Error*: For each decrypted element, we compute the relative error:

$$\epsilon_i = \frac{|y_i - x_i|}{|x_i|}$$

Results are classified into four categories based on the relative error ϵ_i , with each category corresponding to a different tolerance level, which may vary depending on the intended application of FHE:

- 1) **Severe Error** ($\epsilon_i > 10$): the result differs by more than one order of magnitude from the correct value, often rendering it unusable.
- 2) **Significant Error** ($0.1 < \epsilon_i \leq 10$): the result may be unacceptable for precision tasks, but tolerable in coarse-grained applications such as visual representations or robust classification.
- 3) **Moderate Error** ($0.01 < \epsilon_i \leq 0.1$): the deviation is small and potentially acceptable in tasks like statistical analysis or machine learning where high fidelity is not required.
- 4) **Low Error** ($\epsilon_i \leq 0.01$): the result is nearly indistinguishable from the correct value and is considered acceptably decrypted for most practical purposes.

V. EXPERIMENTAL RESULTS

This section presents the results obtained by injecting individual bit-flips during encryption in the CKKS scheme, as described in Section IV, with the goal of evaluating the scheme's resilience against hardware- or software-induced faults.

Experimental campaigns were carried out using both HEAAN 1.0 and OpenFHE 1.2.3, in their *vanilla* and optimized configurations (with RNS and NTT).

A. Vanilla CKKS

1) *Evolution of the L_2 norm under Single Bit-Flips*: To deepen the comparison, we repeated the experiments with HEAAN 1.0, obtaining results that match our theoretical predictions closely. This direct comparison between HEAAN and OpenFHE revealed a marked difference between the *vanilla* implementation and the fully optimized variant with RNS and NTT: the latter exhibits noticeably greater sensitivity to bit-flips, as evidenced by higher L_2 error magnitudes across most bit positions. To isolate the effect of these optimizations, we therefore configured OpenFHE in a simulated *vanilla* mode by disabling both NTT and RNS, as described in Sec. IV-B.

In order to validate this simulation, we ran both HEAAN and OpenFHE (vanilla) under identical conditions. Because OpenFHE only accepts real inputs, we also restricted HEAAN accordingly to real inputs and, after decryption, considered only the real part of each result. This ensured a homogeneous comparison between the two libraries and confirmed that OpenFHE (vanilla) faithfully reproduces the behavior of HEAAN 1.0, in both trend and magnitude.

Figure 7 shows the case of OpenFHE simulated as CKKS vanilla.

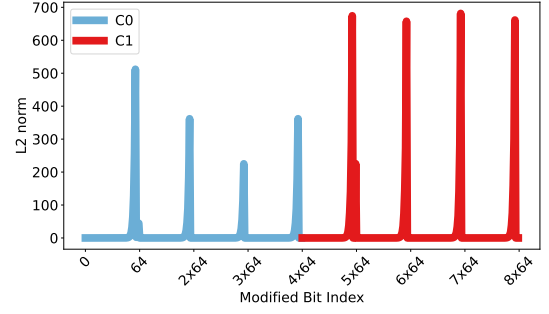


Fig. 7: Impact of a single-bit flip during encryption in OpenFHE without RNS or NTT. The horizontal axis indicates the position of the flipped bit within the ciphertext, while the vertical axis shows the resulting L_2 norm of the decoding error. Parameters: 60-bit modulus, scaling factor $\Delta = 2^{50}$, and ring dimension $N = 4$.

We observe that, for the first polynomial c_0 , the behavior mirrors the theoretical analysis in Fig. 4: the least significant bits exhibit higher robustness against bit-flips, followed by an exponential increase in error magnitude.

In the case of OpenFHE, the expected absolute robustness at coefficient $N/2$ does not hold. During decoding, the coefficient vector prior to the DFT (a specialized FFT) is injected with Gaussian noise affecting both its real and imaginary components. This noise injection is a security measure to thwart key-recovery attacks.

The introduced Gaussian noise has a standard deviation corresponding to the dispersion of the imaginary part of the vector being transformed, which—by properties of the scheme—also follows a Gaussian distribution. Flipping any bit of any coefficient, including the $N/2$ coefficient, increases this noise standard deviation, especially when higher-order bits are modified, leading to increased noise variance that propagates across all elements of the vector, significantly altering the final output and negating the robustness at $N/2$.

We experimentally confirmed that, when this noise injection is disabled, the observed behavior aligns with theoretical expectations: the coefficient $N/2$ of c_0 becomes robust to bit-flips. Conversely, since HEAAN 1.0 does not perform this noise injection, its sensitivity matches the theory exactly.

2) *Impact of the Scaling Factor on Error Categorization*: One of the fundamental parameters of the CKKS scheme is the scaling factor Δ . As analyzed in Sec. III, increasing Δ reduces the relative impact of a single-bit flip during encoding or encryption and also increases the proportion of bits that remain resilient to such faults.

To investigate this effect in practice, we repeated the previous single-bit-flip analysis using four different scaling factors, namely $\Delta \in \{2^{20}, 2^{30}, 2^{40}, 2^{50}\}$. Figure 8 shows the L_2 norm of the decoding error for a bit flip in the first ciphertext polynomial c_0 when running OpenFHE in simulated vanilla mode (i.e., with RNS and NTT disabled). For clarity, only results for c_0 are shown, since the behavior for c_1 is analogous.

We observe that higher values of Δ yield lower L_2 norms after a bit flip, indicating stronger attenuation of induced errors. Furthermore, the point at which the error norm begins

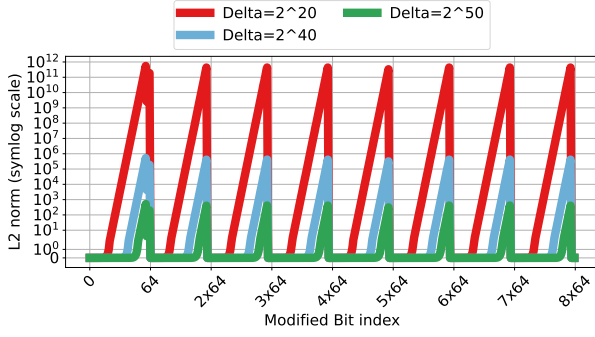


Fig. 8: Impact of a single-bit flip during encryption in OpenFHE without RNS or NTT. The x-axis indicates the bit position in ciphertext c_0 , while the y-axis shows the resulting L_2 norm of the decoding error on a symmetric log scale. Parameters: 60-bit modulus, scaling factors $\Delta = 2^{20}, 2^{30}, 2^{40}, 2^{50}$, and ring dimension $N = 8$.

its exponential growth shifts in alignment with the magnitude of Δ , confirming that larger scaling factors increase the number of error-resilient bit in each coefficient's representation.

To provide a clearer interpretation, we then applied our second metric from Sec. IV, classifying each decryption outcome into three categories based on the fraction of slots correctly recovered (relative error $< 1\%$):

- **Tail:** $> 99\%$ of slots correct
- **Middle:** $1\% - 99\%$ of slots correct
- **Head:** $< 1\%$ of slots correct

For this experiment, we adopted a realistic setting with ring dimension $N = 2^{13} = 8192$ (i.e., 4096 encrypted slots). For each $\Delta \in \{2^{20}, 2^{30}, 2^{40}, 2^{50}\}$ and each single-bit flip, we counted how many slots were correctly decrypted and assigned the result to one of the three categories. Figure 9 presents a histogram of the category frequencies for each scaling factor.

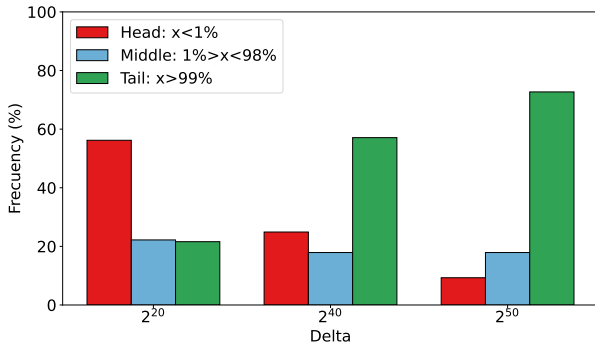


Fig. 9: Histogram of error-categorization outcomes for different scaling factors. Each group of bars corresponds to a specific Δ , showing the percentage of trials in the **Tail** ($> 99\%$ correct), **Middle** ($1\% - 99\%$), and **Head** ($< 1\%$) categories, across all single-bit-flip experiments.

This distribution follows a bimodal ‘all-or-nothing’ pattern: in over 80% of the cases, either more than 99% or fewer than 1% of the slots are correctly decrypted. Importantly, as Δ increases, the frequency of **Tail** outcomes also increases,

demonstrating that a larger scaling factor yields a greater number of bits that the scheme can tolerate without significant error.”

3) *Effect of the Effective Representation Range on Error Categorization:* We now analyze the impact of the effective dynamic range of the input data representation. We fix $\Delta = 2^{20}$, which allows for a wider input range. Recall that the number of bits available for the integer part is approximately given by $q_0 - \Delta$. The effective dynamic range refers to the ratio between the largest and smallest values that can be represented in fixed-point encoding. In our experiments, this range is controlled indirectly by limiting the number of bits allocated to the fractional part of the input values.

In this case, with $q_0 = 60$ bit, the resulting effective input dynamic range is approximately 40 bit. Figure 10 shows histograms of the error category distributions for different input ranges, corresponding to the intervals $[2^9, 2^{10}]$, $[2^{19}, 2^{20}]$ y $[2^{29}, 2^{30}]$. We deliberately avoided using the full 40-bit range, since—as noted earlier—this is only an approximate upper bound, and at that limit, even unmodified input values can fail to decrypt correctly due to overflow.

In all experiments, we used the following parameters: ring dimension $N = 8192$, ciphertext modulus $q_0 = 60$ bit, and scaling factor $\Delta = 2^{20}$.

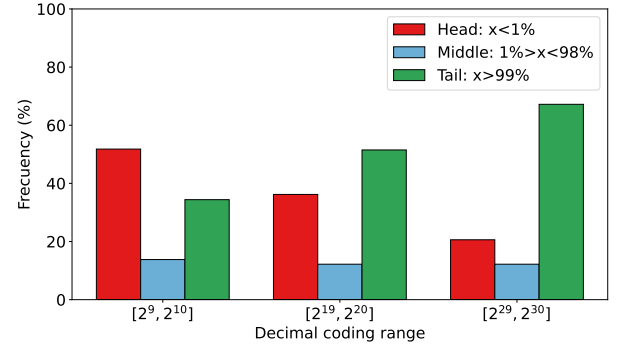


Fig. 10: Histogram showing the percentage of cases in which all elements were correctly decrypted (error $< 1\%$) and the percentage of cases in which all elements were incorrectly decrypted (error $> 1000\%$), for different values of dynamic range: 1, 10, 20, and 30 bits. Each bin corresponds to a specific dynamic range value, and the bars indicate how frequently each outcome occurred across bit-flip experiments.

We observe behavior similar to the impact of the scaling factor, as seen in Fig. 9. As we increase the size of the input space, the percentage of correctly decrypted elements increases while the percentage of incorrectly decrypted elements decreases. If the size of input elements grows while maintaining a fixed scaling factor, this allows representing values with greater relative precision compared to the existing noise.

4) *Effect of reducing the number of encrypted elements:* As noted previously, CKKS can encode up to $N/2$ slots, where N is the ring degree (a power of two). When we encode fewer slots—still a power of two—we observe that additional coefficients remain unaffected by single-bit flips. Figure 11 shows results for $N = 16$ with only $N/4 = 4$ encrypted slots,

allowing us to inspect a larger set of coefficients and evaluate their sensitivity.

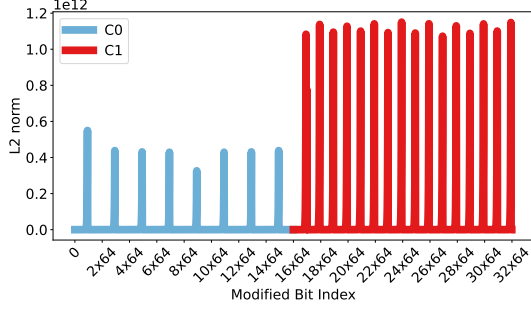


Fig. 11: Impact of a single-bit flip during encryption in OpenFHE without RNS or NTT. The horizontal axis indicates the bit position in the ciphertext, while the vertical axis shows the resulting L_2 norm of the decoding error. Parameters: 60-bit modulus, scaling factor $\Delta = 2^{20}$, ring dimension $N = 16$, and 4 encrypted slots.

The results reveal that odd-indexed coefficients of polynomial c_0 remain unchanged under bit-flips, whereas even-indexed coefficients exhibit the same sensitivity patterns observed earlier.

This phenomenon stems from CKKS’s decoding process in both OpenFHE and HEAAN. As explained in Sec. II, the ratio between the maximum number of slots ($N/2$) and the number actually used defines an interval—termed the *gap*—between the coefficients participating in the inverse transform. During the “special” FFT, only coefficients whose indices are multiples of this gap are considered and scaled in the input vector (see Sec. I for details).

Consequently, when encoding $N/2$ slots, all N coefficients of c_0 are sensitive to bit-flips; encoding $N/4$ slots reduces the number of sensitive coefficients of c_0 to $N/2$; and so on. In the case of c_1 , no matter the number of slots used, all coefficients are sensitive to bit changes. Experimental campaigns confirm that our OpenFHE vanilla simulation (with RNS and NTT disabled) matches the expected behavior.

B. Resilience under an intermediate RNS mode without NTT

We next conducted experimental campaigns to assess CKKS’s sensitivity when using only one of the numeric optimizations—either NTT or RNS. In both pure-NTT and pure-RNS configurations, any single-bit flip caused decryption errors of unacceptable magnitude. As shown in our theoretical analysis, bit flips under RNS produce errors several orders of magnitude larger than under NTT, while NTT alone still yields extremely large errors that preclude practical precision.

An interesting case emerges when CKKS is run with RNS only and the number of encrypted slots is halved or more. Figure 12 reports results for ring dimension $N = 16$ with only 4 encrypted slots (i.e., one power-of-two below the maximum), scaling factor $\Delta = 2^{20}$, and 8-bit input values.

We observe that *odd*-indexed coefficients of c_0 remain fully robust: all their slots decrypt correctly with error below 1%. Any bit flip in an *even*-indexed coefficient, however, causes

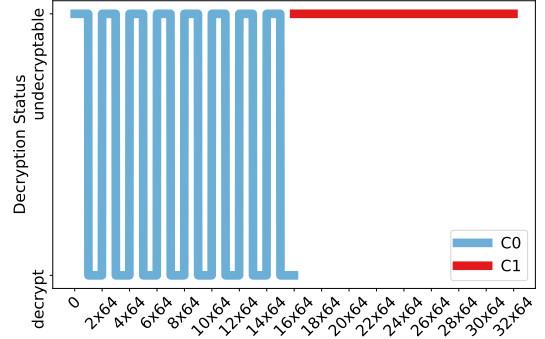


Fig. 12: Impact of a single-bit flip during encryption in OpenFHE without NTT but with two-limb RNS. The horizontal axis indicates the flipped bit position; the vertical axis denotes whether decoding succeeded ($< 1\%$ error) or failed ($> 1000\%$ error). Parameters: 60-bit modulus, $\Delta = 2^{20}$, $N = 16$, and 4 encrypted slots.

decoding failures with errors exceeding 1000%. The number of sensitive coefficients exactly matches the “gap” analysis from Sec. V-A4.

Polynomial c_1 exhibits no robust bits at all: every bit flip causes uniform decoding failure, so its error-categorization histogram is flat and standard deviation is zero.

These results demonstrate that running CKKS with RNS only—together with a non-maximal but non-zero gap—can concentrate robustness on a subset of coefficients. Such a configuration suggests a trade-off between ring utilization and fault resilience. Future work may explore tailored RNS and NTT parameterizations to minimize sensitivity to bit flips while preserving sufficient slot capacity, laying the groundwork for error-reduction strategies in homomorphic encryption schemes that balance precision and fault tolerance.”

C. Summary and Comparison

We provide a high-level comparison of the different CKKS configurations evaluated in this work. For each scenario, we highlight the key resilience pattern and any notable observations.

• Vanilla CKKS:

- Least-significant bits exhibit robustness; error grows exponentially for higher bits.
- Coefficient $N/2$ robust in HEAAN 1.0 but not in OpenFHE vanilla (due to Gaussian noise injection).

• Varying Δ :

- Larger Δ delays the onset of exponential error growth to more significant bits.
- $\Delta \geq 2^{30}$ yields **Tail** outcomes in over 80% of trials.

• Effective Representation Range:

- Increasing integer-part range raises **Tail** frequency and reduces **Head** frequency.
- Behavior parallels that of increasing Δ .

• Reduced Slots:

- Encoding fewer slots reduce the number of sensitive coefficients in c_0 .

• RNS without NTT:

- Some coefficients of c_0 remain robust; all flips in c_1 fail.
- Demonstrates a “gap”-driven concentration of robustness when using RNS only.

This concise overview highlights how each parameter adjustment—from vanilla through optimized variants—modulates CKKS’s fault tolerance, guiding practical parameter selection under two-column constraints.

VI. CONCLUSIONS

This paper has presented a comprehensive evaluation of CKKS’s sensitivity to single-bit flips, emphasizing the influence of RNS and NTT optimizations on error resilience. While the vanilla CKKS implementation exhibits substantial innate tolerance to individual bit-flip faults, the optimized variants—with RNS or NTT enabled—display markedly increased vulnerability, potentially undermining the correctness of decrypted outputs.

Our findings indicate that, despite its performance drawbacks, vanilla CKKS offers a robustness advantage by minimizing the impact of isolated bit errors compared to its optimized counterparts. Furthermore, when employing large ring dimensions for security, encoding fewer slots (powers of two below the maximum) introduces redundancy that renders a subset of coefficients entirely insensitive to bit flips. This “gap”-driven effect persists even in optimized configurations, highlighting a practical mechanism for enhancing resilience without altering core codec operations.

Overall, these results deepen our understanding of fault tolerance in homomorphic encryption schemes and provide actionable guidance for balancing throughput, security, and error resilience when selecting CKKS parameters.

a) *Future Work:* Promising directions include studying error tolerance in application-specific domains—such as deep neural networks for image processing, where limited accuracy loss is acceptable—and conducting a detailed investigation of error propagation under multiple concurrent bit flips. Such analyses will further illuminate strategies for error mitigation in practical homomorphic computing scenarios.

ACKNOWLEDGMENTS

First, I would like to thank Pradip Bose, whose inspiration to explore fault tolerance in homomorphic encryption significantly shaped this work. I also appreciate the open-source homomorphic encryption community and the developers of the OpenFHE and SEAL libraries, whose tools and documentation greatly facilitated our experiments. In particular, I extend my gratitude to Ahmad Al Badawi for his help setting up OpenFHE correctly and for his clear explanations and references on CKKS encoding and decoding.

REFERENCES

- [1] R. L. Rivest, A. Shamir, and L. Adleman, “A method for obtaining digital signatures and public-key cryptosystems,” *Communications of the ACM*, vol. 21, no. 2, p. 120–126, Feb. 1978.
- [2] C. Gentry, S. Halevi, and N. P. Smart, “Homomorphic evaluation of the AES circuit,” in *Proceedings of the Annual Cryptology Conference (CRYPTO)*, R. Safavi-Naini and R. Canetti, Eds., vol. 7417. Berlin, Heidelberg: Springer Berlin Heidelberg, 2012, pp. 850–867.
- [3] J. H. Cheon, K. Han, A. Kim, M. Kim, and Y. Song, “A full rns variant of approximate homomorphic encryption,” in *Proceedings of the International Conference on Selected Areas in Cryptography (SAC)*, C. Cid and M. J. Jacobson Jr., Eds., vol. 11349. Cham: Springer International Publishing, 2019, pp. 347–368.
- [4] A. Kim, A. Papadimitriou, and Y. Polyakov, “Approximate homomorphic encryption with reduced approximation error,” in *Proceedings of the Cryptographers’ Track at the RSA Conference*, S. D. Galbraith, Ed., vol. 13161. Cham: Springer International Publishing, 2022, pp. 120–144.
- [5] E. Lee, J.-W. Lee, Y.-S. Kim, and J.-S. No, “Optimization of homomorphic comparison algorithm on rns-ckks scheme,” *IEEE Access*, vol. 10, pp. 26 163–26 176, 2022.
- [6] H. Kwon, H. Lee, G. Jung, and Y. Lee, “Energy-efficient flexible RNS-CKKS processor for FHE-based privacy-preserving computing,” *IEEE Journal of Solid-State Circuits*, vol. 60, no. 1, pp. 136–145, 2024.
- [7] X. Deng, S. Fan, Z. Hu, Z. Tian, Z. Yang, J. Yu, D. Cao, D. Meng, R. Hou, M. Li *et al.*, “Trinity: A general purpose fhe accelerator,” in *Proceedings of the IEEE/ACM International Symposium on Microarchitecture (MICRO)*, Institute of Electrical and Electronics Engineers, Inc. Los Alamitos, CA, USA: IEEE Computer Society, 2024, pp. 338–351.
- [8] N. Samardzic, A. Feldmann, A. Krastev, S. Devadas, R. Dreslinski, C. Peikert, and D. Sanchez, “F1: A fast and programmable accelerator for fully homomorphic encryption,” in *Proceedings of the Annual IEEE/ACM International Symposium on Microarchitecture (MICRO)*. New York, NY, USA: Association for Computing Machinery, 2021, pp. 238–252.
- [9] J. Ma, S.-A. Naas, S. Sigg, and X. Lyu, “Privacy-preserving federated learning based on multi-key homomorphic encryption,” *International Journal of Intelligent Systems*, vol. 37, no. 9, pp. 5880–5901, 2022.
- [10] M. Zhang, L. Wang, X. Zhang, Z. Liu, Y. Wang, and H. Bao, “Efficient clustering on encrypted data,” in *Applied Cryptography and Network Security*, C. Pöpper and L. Batina, Eds. Cham: Springer Nature Switzerland, 2024, pp. 213–236.
- [11] Y. Zhang, Y. Miao, X. Li, L. Wei, Z. Liu, K.-K. R. Choo, and R. H. Deng, “Efficient privacy-preserving federated learning with improved compressed sensing,” *IEEE Transactions on Industrial Informatics*, vol. 20, no. 3, pp. 3316–3326, 2023.
- [12] F. Sabath, *Classification of Electromagnetic Effects at System Level*. New York, NY: Springer New York, NY, 2010, pp. 325–333. [Online]. Available: https://doi.org/10.1007/978-0-387-77845-7_38
- [13] T. Kolditz, T. Kissinger, B. Schlegel, D. Habich, and W. Lehner, “Online bit flip detection for in-memory b-trees on unreliable hardware,” in *Proceedings of the Tenth International Workshop on Data Management on New Hardware*, ser. DaMoN ’14. New York, NY, USA: Association for Computing Machinery, 2014, pp. 1–9.
- [14] O. Mutlu and J. S. Kim, “Rowhammer: A retrospective,” *IEEE Transactions on Computer-Aided Design of Integrated Circuits and Systems*, vol. 39, no. 8, pp. 1555–1571, 2019.
- [15] K.-J. Li, Y.-Z. Xie, F. Zhang, and Y.-H. Chen, “Statistical inference of serial communication errors caused by repetitive electromagnetic disturbances,” *IEEE Transactions on Electromagnetic Compatibility*, vol. 62, no. 4, pp. 1160–1168, 2020.
- [16] Z. Li, H. Menon, D. Maljovec, Y. Livnat, S. Liu, K. Mohror, P.-T. Bremer, and V. Pascucci, “Spotsdc: Revealing the silent data corruption propagation in high-performance computing systems,” *IEEE Transactions on Visualization and Computer Graphics*, vol. 27, no. 10, pp. 3938–3952, 2020.
- [17] S. K. Höeffgen, S. Metzger, and M. Steffens, “Investigating the effects of cosmic rays on space electronics,” *Frontiers in Physics*, vol. 8, p. 318, 2020.
- [18] H. Dixit, “Silent data corruptions at scale,” in *Proceedings of the International Symposium on On-Line Testing and Robust System Design (IOLTS)*. Institute of Electrical and Electronics Engineers, Inc, 2023, pp. 1–2.
- [19] D. J. Bernstein, “The tangent fft,” in *International Symposium of Applied Algebra, Algebraic Algorithms and Error-Correcting Codes (AAECC)*, S. Boztaş and H.-F. F. Lu, Eds. Berlin, Heidelberg: Springer Berlin Heidelberg, 2007, pp. 291–300.
- [20] —, *Fast multiplication and its applications*, ser. Mathematical Sciences Research Institute Publications. United Kingdom: Cambridge University Press, 2008, pp. 325–384. [Online]. Available: <https://library.slmath.org/books/Book44/files/10bern.pdf>

- [21] V. Lyubashevsky, C. Peikert, and O. Regev, “A toolkit for ring-lwe cryptography,” in *Proceedings of the Annual International Conference on the theory and applications of cryptographic techniques (EUROCRYPT)*, vol. 7881. Berlin, Heidelberg: Springer, 2013, pp. 35–54.
- [22] A. Costache, B. R. Curtis, E. Hales, S. Murphy, T. Ogilvie, and R. Player, “On the precision loss in approximate homomorphic encryption,” in *Proceedings of the International Conference on Selected Areas in Cryptography (SAC)*. Berlin, Heidelberg: Springer-Verlag, 2024, p. 325–345.
- [23] V. van der Leest, G.-J. Schrijen, H. Handschuh, and P. Tuyls, “Hardware intrinsic security from d flip-flops,” in *Proceedings of the Fifth ACM Workshop on Scalable Trusted Computing*, ser. STC '10. New York, NY, USA: Association for Computing Machinery, Oct. 2010, p. 53–62.
- [24] J. F. Ziegler and W. A. Lanford, “Effect of cosmic rays on computer memories,” *Science*, vol. 206, no. 4420, pp. 776–788, 1979.
- [25] P. V. A. Mohan, *Residue Number Systems: Theory and Applications*. Birkhäuser Chama, 2016.
- [26] A. A. Badawi, A. Alexandru, J. Bates, F. Bergamaschi, D. B. Cousins, S. Erabelli, N. Genise, S. Halevi, H. Hunt, A. Kim, Y. Lee, Z. Liu, D. Micciancio, C. Pascoe, Y. Polyakov, I. Quah, S. R.V., K. Rohloff, J. Saylor, D. Saponitsky, M. Triplett, V. Vaikuntanathan, and V. Zucca, “OpenFHE: Open-source fully homomorphic encryption library,” Cryptology ePrint Archive, Paper 2022/915, 2022. [Online]. Available: <https://eprint.iacr.org/2022/915>